The final publication is available at Elsevier via http://dx.doi.org/10.1016/j.mbs.2021.108591. © 2021. This manuscript version is made available under the CC-BY-NC-ND 4.0 license http://creativecommons.org/licenses/by-nc-nd/4.0/

Mathematical Biosciences 336 (2021) 108591

Contents lists available at ScienceDirect

Mathematical Biosciences

journal homepage: www.elsevier.com/locate/mbs

Original Research Article

# Spatially localized cluster solutions in inhibitory neural networks

Hwayeon Ryu [a,*], Jennifer Miller [b,1], Zeynep Teymuroglu [c], Xueying Wang [d], Victoria Booth [e], Sue Ann Campbell [f]

[a] Department of Mathematics and Statistics, Elon University, Elon, NC, USA
[b] Mathematics Department, Bellarmine University, Louisville, KY, USA
[c] Department of Mathematics and Computer Science, Rollins College, Winter Park, FL, USA
[d] Department of Mathematics and Statistics, Washington State University, Pullman, WA, USA
[e] Departments of Mathematics and Anesthesiology, University of Michigan, Ann Arbor, MI, USA
[f] Department of Applied Mathematics and Centre for Theoretical Neuroscience, University of Waterloo, Waterloo ON, Canada

ARTICLE INFO

*MSC:*
92B20
92B25
34D20

*Keywords:*
Inhibitory networks
Connectivity
Clusters
Phase model

ABSTRACT

Neurons in the inhibitory network of the striatum display cell assembly firing patterns which recent results suggest may consist of spatially compact neural clusters. Previous computational modeling of striatal neural networks has indicated that non-monotonic, distance-dependent coupling may promote spatially localized cluster firing. Here, we identify conditions for the existence and stability of cluster firing solutions in which clusters consist of spatially adjacent neurons in inhibitory neural networks. We consider simple non-monotonic, distance-dependent connectivity schemes in weakly coupled 1-D networks where cells make stronger connections with their $k$th nearest neighbors on each side and weaker connections with closer neighbors. Using the phase model reduction of the network system, we prove the existence of cluster solutions where neurons that are spatially close together are also synchronized in the same cluster, and find stability conditions for these solutions. Our analysis predicts the long-term behavior for networks of neurons, and we confirm our results by numerical simulations of biophysical neuron network models. Our results demonstrate that an inhibitory network with non-monotonic, distance-dependent connectivity can exhibit cluster solutions where adjacent cells fire together.

## 1. Introduction

Many types of brain activity are characterized by coordinated activity of neural assemblies, in which neuron firing is synchronized within an individual assembly but not between different assemblies [1–6]. Neural assemblies have been observed between neurons in different cortical columns [3], within regions of the hippocampus [2,4], the dentate gyrus [6], and between cells in the striatum [1,7,8] and the olfactory bulb [5]. Neural assemblies may involve neurons which are widespread across one or more brain regions [3,4] or may involve spatially localized neurons [1,6]. Understanding the dynamics and formation of neuronal assemblies within larger neural networks has gained increasing importance in neuroscience [9] and has been studied both experimentally [1,4–6,10] and using computational modeling [11–18].

In neural network models, the formation of neural assemblies has been analyzed by identifying cluster solutions in networks of intrinsically oscillating neurons [10,14–17,19,20]. Clustering defines a type of solution where the network of oscillators breaks into subgroups. Within each subgroup, the phases of the oscillators are the same, while oscillators in different subgroups are phase-locked with some nonzero phase difference. A useful mathematical framework for studying cluster solutions is the phase model reduction [21,22]. This framework has been used to study synchronization and clustering in a variety of coupled oscillator networks [23–27]. Another useful approach is to consider a continuum model representing the limit of an infinite number of oscillators [28,29]. Such models are represented as partial differential equations and cluster solutions correspond to wave-like solutions, sometimes called twisted states [28,30–33].

Cluster solutions have been extensively studied in models with all-to-all identical coupling [23,24,29,34–36]. In particular, the existence and stability of two cluster states where there can be a different number of neurons in each cluster has been studied in depth for the all-to-all coupling case [35,36].

A limited number of papers have studied cluster solutions in models with structured connectivity. These papers primarily focus on networks with neurons arranged in a 1-dimensional ring, of arbitrary

* Corresponding author.
*E-mail addresses:* hryu@elon.edu (H. Ryu), jmiller@bellarmine.edu (J. Miller), zteymuroglu@rollins.edu (Z. Teymuroglu), xueying.wang@wsu.edu (X. Wang), vbooth@med.umich.edu (V. Booth), sacampbell@uwaterloo.ca (S.A. Campbell).
[1] Co-first author.

https://doi.org/10.1016/j.mbs.2021.108591
Received 30 July 2020; Received in revised form 10 March 2021; Accepted 11 March 2021
Available online 26 March 2021
0025-5564/© 2021 Elsevier Inc. All rights reserved.

size. In [31,36] a phase model representing a system with all-to-all identical synaptic coupling and local (nearest neighbor) gap-junctional coupling is formulated. They study how the gap-junctional coupling can induce a shift from synchronous or two cluster solutions to the splay state ($N$-cluster solution). In [30,32] the existence and stability of cluster solutions is studied in a continuum model where each oscillator has identical coupling to a subset of its nearest neighbors. In [33] a continuum model with local excitation and lateral inhibition is used to show the transition from stable synchrony with no inhibition to traveling wave solution with large inhibition. Both 1-dimensional and 2-dimensional models are studied. In our previous work [19,20], we used the phase model approach to determine existence and stability conditions for cluster solutions in networks with various connectivity schemes. As in many other studies [23,24], all of the work cited above focused on cluster solutions where the phase difference between any two adjacent neurons in the network is the same. Thus, cells in the same cluster were dispersed throughout the network.

Neural assembly firing has been identified in the striatum, a sparsely connected, inhibitory network that is part of the basal ganglia circuit [1,7,8,37,38]. Recent experimental imaging of inhibitory medium spiny neuron firing in the striatum has suggested that assemblies can be spatially compact [1]. While computational modeling of inhibitory striatal networks has primarily investigated the formation of neural assemblies in which the assembly cells are spatially dispersed in the network [12,18], a recent study found that spatially compact cluster firing patterns can result from non-monotonic, distance-dependent connectivity in which cells made stronger synaptic connections with their more spatially distant neighbors compared to their nearest neighbors [39]. This result suggests that in inhibitory networks neurons located near one another should be able to be a part of the same cluster when they are more strongly connected to neighbors farther away.

In this work, motivated by the results in [39], we study 1-D ring, inhibitory networks with simple non-monotonic, distance-dependent connectivity schemes. Specifically, we consider networks in which neurons are connected to only their $k$th nearest neighbors and identify conditions for the existence and stability of solutions which exhibit spatially localized cluster firing. We additionally consider connectivity schemes with connections between the first to $(k-1)$th nearest neighbors that are weaker than connections to $k$th nearest neighbors, and analyze how this additional local coupling between cells affects the existence and stability of spatially localized cluster solutions. We employ a phase model reduction of the network to obtain analytical conditions and then test the conditions with numerical simulations of biophysical neural network models.

Our paper is structured as follows: Section 2 provides the description of the methodology we employ, including the phase model reduction (Section 2.1) for analysis and the biophysical neuron model (Section 2.2) for numerical simulations. Section 3 describes our analysis. Section 4 describes our numerical simulations. We conclude with a discussion of our results in Section 5.

## 2. Methodology

We begin by reviewing the phase reduction method that reduces a weakly coupled neural network model to a phase model. This phase model is used to conduct our analysis. We then introduce the specific neural network model that we use for numerical simulations and include the parameter values for our simulations.

### 2.1. Phase reduction method

Consider a general network model consisting of $N$ identical, weakly coupled oscillators on a ring with circulant coupling

$$\frac{dX_i}{dt} = F(X_i(t)) + \epsilon \sum_{j=1}^{N} W_{ij} G(X_i, X_j), \quad X_i \in \mathbb{R}^n, \quad 1 \le i \le N, \tag{1}$$

where $\epsilon$ is the coupling strength with $0 < \epsilon \ll 1$, $F$ is the vector field of the isolated neuron, $G$ is the coupling function and $W = (W_{ij})$ is the coupling matrix with $W_{ij} = g_{j-i \pmod N}$ and $W_{ii} = 0$ for $i, j = 1, 2, \dots, N$.

We assume that when isolated from the network each neuron exhibits an exponentially asymptotically stable $T$-periodic orbit, denoted as $\hat{X}(t)$, for $0 \le t \le T = \frac{2\pi}{\Omega}$, which is a solution of

$$\frac{dX}{dt} = F(X(t)), \qquad X \in \mathbb{R}^n. \tag{2}$$

Applying the theory of weakly coupled oscillators [21,22,40], the complete state of each neuron in the network can be approximated by its phase on its $T$-periodic limit cycle, $\theta_i(t) = \Omega t + \varphi_i(t) \in [0, 2\pi)$, where $\varphi_i(t)$ is the relative phase of the $i$th neuron. Hence, this theory enables us to significantly reduce the number of equations that describe a neuronal network from $n$ equations to one per neuron.

The dynamics of the relative phase of the $i$th neuronal oscillator is slowly varying and governed by the equation

$$\frac{d\varphi_i}{dt} = \epsilon \sum_{j=1}^{N} W_{ij} H(\theta_j(t) - \theta_i(t)). \tag{3}$$

Here $H$ is known as the interaction function and is given by

$$H(\theta_j - \theta_i) = \frac{1}{T} \int_0^T Z(t) G[\hat{X}(t), \hat{X}(t + (\theta_j - \theta_i)/\Omega)] dt. \tag{4}$$

$H$ captures the modulation of the instantaneous phase of the $i$th oscillator due to the coupling. $Z$ is referred to as the phase response curve of the unperturbed oscillator, which is the unique periodic solution of the linearized adjoint system

$$\frac{dZ}{dt} = -[DF(\hat{X}(t))]^T Z,$$

subject to the normalization condition

$$\frac{1}{T} \int_0^T Z(t) \cdot F(\hat{X}(t)) dt = 1.$$

Thus, the corresponding phase model is given by

$$\frac{d\theta_i}{dt} = \Omega + \epsilon \sum_{j=1}^{N} W_{ij} H(\theta_j(t) - \theta_i(t)), \quad 1 \le i \le N. \tag{5}$$

In view of circulant coupling ($W_{ij} = g_{j-i \pmod N}$ for $1 \le i, j \le N$) and no self-coupling ($W_{ii} = g_0 = 0$, $1 \le i \le N$), the phase model (5) can be written as

$$\frac{d\theta_i}{dt} = \Omega + \epsilon \sum_{k=1}^{N-1} g_k H(\theta_{(i+k) \bmod N} - \theta_i), \quad 1 \le i \le N. \tag{6}$$

We will use this phase model to determine the existence and stability of certain cluster solutions and how this depends on the connections $g_k$, focusing on results that can be applied to any neural model (1). We then use these results to predict which cluster solutions will be stable in the neural network model described below.

### 2.2. Neural network model

To verify our analysis results, we numerically simulate networks of neurons modeled by the conductance-based Wang and Buzsáki inhibitory interneuron model [41]. This model uses the classic Hodgkin–Huxley formalism [42] with parameters adjusted to match the action potential shape and spiking properties of fast-spiking interneurons. The membrane voltage $V$ of each individual neuron is governed by the following equations:

$$\begin{aligned} C\frac{dV}{dt} &= I_{app} - g_{Na} m_\infty^3(V) h (V - V_{Na}) - g_K n^4 (V - V_K) - g_L (V - V_L) \\ &= I_{app} - I_{ion}(V, h, n) = f^V(V, h, n), \\ \frac{dh}{dt} &= \gamma(\alpha_h(V)(1 - h) - \beta_h(V) h) = f^h(V, h), \\ \frac{dn}{dt} &= \gamma(\alpha_n(V)(1 - n) - \beta_n(V) n) = f^n(V, n), \end{aligned} \tag{7}$$

**Table 1**
Description of parameters and the values used for the neuron model in (8).

| Parameter | Description | Value |
|---|---|---|
| $\gamma$ | Adjusts reaction rates for temperature | 5 |
| $g_{Na}$ | Maximal sodium conductance | 35 mS/cm$^2$ |
| $g_K$ | Maximal potassium conductance | 9 mS/cm$^2$ |
| $g_L$ | Maximal leak conductance | 0.1 mS/cm$^2$ |
| $V_{Na}$ | Sodium reversal potential | 55 mV |
| $V_K$ | Potassium reversal potential | −90 mV |
| $V_L$ | Leak reversal potential | −65 mV |
| $C$ | Membrane capacitance | 1 μF/cm$^2$ |
| $I_{app}$ | Applied current | 0.4 μA/cm$^2$ |
| $V_{syn}$ | Synapse reversal potential | −75 mV |
| $g_{syn}$ | Maximal synaptic conductance | 0.05 mS/cm$^2$ |
| $\alpha_0$ | Synaptic maximal activation rate | 4 ms$^{-1}$ |
| $\tau_{inh}$ | Synaptic decay time | 2 ms |

where $t$ is time in mS and $V$ is the cell membrane potential in mV. The variables $h$ and $n$ are, respectively, the inactivation gating of the sodium current and the activation gating of the potassium current. The sodium current is assumed to instantaneously activate according to the steady state activation function $m_\infty(V) = \alpha_m(V)/(\alpha_m(V)+\beta_m(V))$, where $\alpha_m(V) = -0.1(V+35)/(\exp(-0.1(V+35))-1)$, $\beta_m(V) = 4\exp(-(V+60)/18)$ are the voltage dependent reaction rates associated with the activation gate with units ms$^{-1}$. The reaction rates for the inactivation of the sodium channel and activation of the potassium channel are given by: $\alpha_h(V) = 0.07\exp(-(V+58)/20)$, $\beta_h(V) = 1/(\exp(-0.1(V+28))+1)$, $\alpha_n(V) = -0.01(V+34)/(\exp(-0.1(V+34))-1)$, $\beta_n(V) = 0.125\exp(-(V+44)/80)$. We model the situation where each neuron is intrinsically firing at a biologically reasonable rate of less than 60 Hz [41,43] by setting $I_{app} < 1$ μA/cm$^2$.

In the network, neurons are coupled with fast inhibitory synapses that are modeled using first order kinetics following [44]:

$$\begin{aligned} C\frac{dV_i}{dt} &= f^V(V_i,h_i,n_i) - g_{syn}(V_i - V_{syn})\sum_{j=1}^{N} W_{ij}s_j,\\ \frac{dh_i}{dt} &= f^h(V_i,h_i),\\ \frac{dn_i}{dt} &= f^n(V_i,n_i),\\ \frac{ds_i}{dt} &= -\frac{s_i}{\tau_{inh}} + \alpha_{inh}(V_i)(1-s_i) = f^s(V_i,s_i), \end{aligned} \tag{8}$$

where $g_{syn}$ is the maximal synaptic strength and $W_{ij}$ scales the strength of the synaptic current from cell $j$ to cell $i$. The synaptic gating variable $s_i$ for presynaptic cell $i$ depends on membrane voltage $V_i$ according to

$$\alpha_{inh}(V) = \alpha_0/(1+\exp(-V/5)).$$

Descriptions of the parameters and values used in our numerical simulations are given in Table 1.

Comparison of numerical results of this interneuron network model with the predictions given by the phase reduction model requires the interaction function $H$ in Eq. (6). The model (8) can be put in the form given in (1) if we identify $\epsilon = g_{syn}$, $X_i = (V_i,h_i,n_i,s_i)^T$, $F = (f^V,f^h,f^n,f^s)^T$ and $G(X_i,X_j) = \big((V_{syn}-V_i)s_j,0,0,0\big)^T$. Then the function $H$ can be computed from (4). For any neural network, $H$ rarely has a closed-form expression and one usually has to resort to numerical evaluation. In this paper, we use XPPAUT [45] to numerically compute $H$ for the Wang–Buzsáki inhibitory network (8).

## 3. Analysis

We look for solutions of (6) that consist of $m$ clusters with $k$ ($1 < k < N$) adjacent neurons synchronized; hence we assume that $N = mkp$ for some $1 \le p < N$. We ignore the case $k = 1$, which corresponds to the case where synchronized cells in a cluster are distributed throughout the network. This case is very well studied and not relevant to the type of solutions we focus on here. To be more precise, define the phase difference $\phi_i = \theta_{(i+1)\bmod N} - \theta_i$, $i = 1,\dots,N$. We look for solutions of (6) of the form

$$\bar\theta_i = (\Omega+\epsilon\omega)t + \theta_{i0}, \tag{9}$$

where

$$\theta_{10} = 0,\ \theta_{i0} = \sum_{j=1}^{i-1}\phi_j, \quad 2 \le i \le N, \tag{10}$$

and

$$\begin{aligned} &\phi_{kq+1} = \phi_{kq+2} = \cdots = \phi_{kq+(k-1)} = 0, \quad q = 0,1,\dots,mp-1,\\ &\phi_{kq+k} = \frac{2\pi l}{m} := \psi_{m,l} := \psi_m, \end{aligned} \tag{11}$$

with $gcd(l,m) = 1$ and $l < m$. Note that $\psi_m$ is the phase difference between adjacent clusters.

As shown in [28, Lemma 3.2], if this $m$-cluster solution exists, sufficient conditions for it to be asymptotically stable are as follows

$$H'(0), H'(\psi_m), H'(2\psi_m), \dots, H'((m-1)\psi_m) > 0, \tag{12}$$

The graph of the matrix $W = \mathrm{circ}[0,g_1,g_2,\dots,g_{N-1}]$ is connected.

Our focus will be on determining conditions for existence, and necessary and sufficient conditions for stability.

### 3.1. Short discussion of a simple case: Decoupled networks

A simple case when the $m$-cluster solutions given by (9)–(11) can occur is when cells are only connected to their $k$th nearest neighbor on either side and the network decouples into $k$ subnetworks. In this case, each subnetwork has $mp$ cells with nearest neighbor coupling. We briefly discuss this case to provide context for our analysis and numerical simulations of other network structures that admit cluster solutions of this type.

To illustrate $m$−cluster solutions in this case, we show two examples for $N = 12$ in Fig. 1. In Fig. 1(a), there are $m = 2$ clusters (cells represented by circular nodes all fire together as one cluster, and those represented by rectangular nodes fire together as the second). The cells have reciprocal, second nearest neighbor coupling, $k = 2$ (e.g., cell 1 is coupled to cells 3 and 11). There are $p = 3$ subgroups in each cluster (e.g., the cluster of cells represented by circular nodes contains three spatially separated subgroups: 1 & 2, 5 & 6, and 9 & 10). The second nearest neighbor coupling causes the network to have two disjoint subnetworks, shown on the right, i.e., odd-numbered vs. even-numbered cells. Fig. 1(b) shows a network solution with the same number of cells but with different connectivity. Each neuron is only coupled to its third nearest neighbor ($k = 3$) on each side and the network of $N = 12$ decomposes into 3 disjoint subnetworks, each containing 4 neurons. In general, $k$th nearest neighbor coupling results in $k$ disjoint subnetworks with $mp$ neurons in each subnetwork.

To analyze existence of $m$-cluster solutions in networks with $N = mkp$ neurons and $g_k > 0$, $g_{N-k} > 0$, and $g_i = 0$ otherwise, we substitute (9)–(11) into (6) to obtain

$$\begin{aligned} \frac{d\bar\theta_i}{dt} &= \Omega + \epsilon\omega = \Omega + \epsilon\left(g_k H(\theta_{i+k,0}-\theta_{i0}) + g_{N-k}H(\theta_{i+N-k,0}-\theta_{i0})\right)\\ &= \Omega + \epsilon\big(g_k H(\psi_m) + g_{N-k}H(-\psi_m)\big). \end{aligned}$$

Thus, $\omega = g_kH(\psi_m) + g_{N-k}H(-\psi_m)$. It is clear that in (11) $\sum_{i=1}^{N}\phi_i = m\psi_m = 0 \bmod 2\pi$, which leads to an $m$-cluster solution in the network of size $N = mkp$.

To analyze stability of this $m$-cluster solution, we consider the linearization of (6) about the solution $\bar\theta_i(t)$ given by

$$\frac{d\vec u}{dt} = \epsilon A\vec u,$$

where $A = circ(a_1,a_2,\dots,a_N)$ with

$$\begin{aligned} &a_1 = -\big(g_kH'(\psi_m) + g_{N-k}H'(-\psi_m)\big), \quad a_{k+1} = g_kH'(\psi_m),\\ &a_{N-k+1} = g_{N-k}H'(-\psi_m), \qquad\qquad a_i = 0 \quad \text{otherwise}. \end{aligned}$$

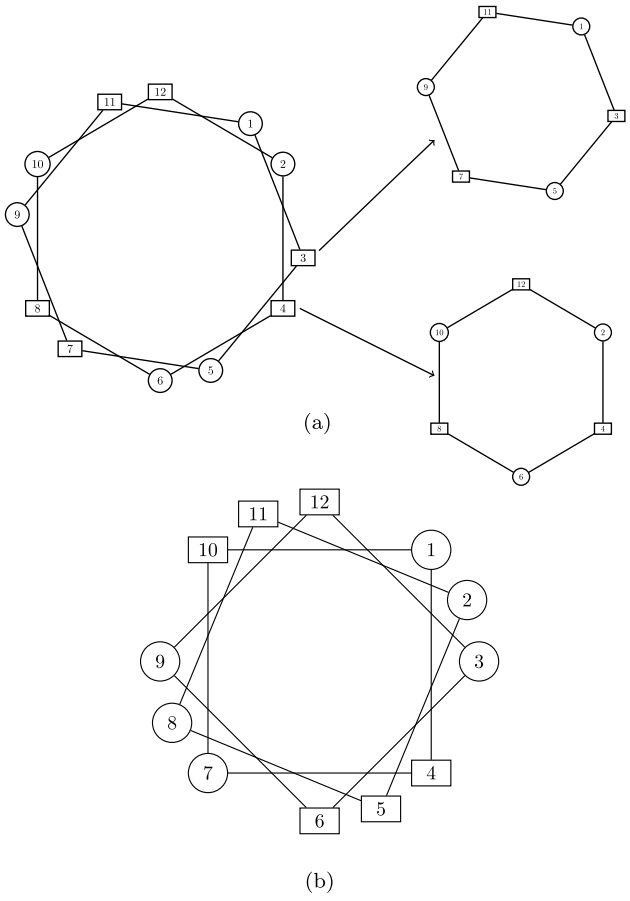


**Fig. 1.** (a) Top: the full network for $N = 12$, $m = 2$, $k = 2$, $p = 3$, which can be decomposed into the two disjoint networks of 6 cells each, i.e., odd-numbered vs. even-numbered cells; (b) Bottom: the network of $N = 12$, $m = 2$, $k = 3$, $p = 2$.

Let $\rho_j = e^{2\pi j\sqrt{-1}/N}$ for $1 \le j \le N$. Because $A$ is circulant and $\rho_j^N = 1$, the eigenvalues of $A$ are given by

$$\begin{aligned}\lambda_j^A &= a_1 + a_{k+1}\rho_j^k + a_{N-k+1}\rho_j^{N-k}\\ &= -\big(g_k H'(\psi_m) + g_{N-k}H'(-\psi_m)\big) + g_k H'(\psi_m)\rho_j^k + g_{N-k}H'(-\psi_m)\rho_j^{-k},\end{aligned}$$

Hence, the real part of the eigenvalues is

$$\Re(\lambda_j^A) = -\big(g_k H'(\psi_m) + g_{N-k}H'(-\psi_m)\big)\left(1 - \cos\frac{2\pi kj}{N}\right), \quad 1 \le j \le N.$$

Note that $\Re(\lambda_j^A) = 0$ whenever $\frac{kj}{N}$ is an integer. Thus there are $k$ zero eigenvalues. Therefore, the $m$-cluster solution defined by (9)–(11) is stable if and only if the following condition is satisfied:

$$g_k H'(\psi_m) + g_{N-k}H'(-\psi_m) > 0. \tag{13}$$

When $g_k = g_{N-k}$, then

$$\Re(\lambda_j^A) = -2g_k H'_{odd}(\psi_m)\left(1 - \cos\frac{2\pi kj}{N}\right), \quad 1 \le j \le N.$$

It follows that this $m$-cluster solution is stable if and only if $H'_{odd}(\psi_m) > 0$.

We note that the existence of $m$-cluster solutions is determined only by the network structure. Additionally, given symmetric connection weights, the stability of the solutions is independent of the network size.

In fact, solutions of the form (9)–(11) correspond to each subnetwork having an $m$-cluster solution where adjacent neurons have a phase difference of $2\pi/m$. Comparison with prior work [20,30] shows that the eigenvalues described above correspond to the eigenvalues of the linearization about this $m$-cluster solution in a network of $mp$ neurons with first nearest neighbor coupling. Each eigenvalue has multiplicity $k$ as there are $k$ subnetworks. The zero eigenvalues correspond to motion along the solutions [19,28]. These eigenvalues mean that small perturbations to the $m$-cluster solutions may lead to other solutions as we now describe.

The solutions discussed above focus on the case where the $k$ disjoint subnetworks are synchronized, namely when cells within each cluster have the same phases (or spike at the same time) or, equivalently, have a zero time shift between them. However, other solutions, where the disjoint subnetworks are not synchronized, will also exist. Such solutions would have phase differences

$$\phi_{kq+1}, \phi_{kq+2}, \dots, \phi_{kq+(k-1)}, \phi_{kq+k} \ge 0, \quad q = 0, 1, \dots, mp-1. \tag{14}$$

For example, consider the situation with $k = 2$, so the network decouples into 2 subnetworks, and assume each subnetwork has a 2-cluster solution. In this case, adjacent cells within the same subnetwork fire in anti-phase, i.e., $\theta_{i+2} - \theta_i = \pi$. Then for any $\alpha$ one can find solutions $\phi_{kq+1} = \theta_{kq+2} - \theta_{kq+1} = \alpha$ and $\phi_{kq+2} = \theta_{kq+3} - \theta_{kq+2} = \pi - \alpha$ for $q = 0, 1, \dots, mp-1$. The value of $\alpha$ is determined by the initial conditions, but the eigenvalues of these solutions are the same as described above.

### 3.2. Effect of other connections

Now we consider the $m$-cluster solutions given by (9)–(11) when cells are connected to their first to $k$th nearest neighbors on either side. We consider different possible strengths of the additional first through $(k-1)$st nearest neighbor coupling, $g_{k-j}, g_{N-j}$, $j = 1, \dots, k-1$, relative to the stronger $k$th nearest neighbor coupling, $g_k, g_{N-k}$.

First we consider the case when all connections which exist are of equal strength, i.e., $O(1)$ with respect to $\epsilon$. In this situation we give sufficient conditions for the existence of cluster solutions.

**Theorem 3.1** (*Strong Additional Coupling*). *Consider the system (6) with $N = mkp$ and coupling matrix defined by*

$$\text{circ}[0, g_1, g_2, \dots, g_k, 0, \dots, 0, g_{N-k}, \dots, g_{N-1}], \tag{15}$$

*where $g_j = O(1)$ with respect to $\epsilon$. The only possible model-independent phase-locked solution with $k$ adjacent neurons synchronized is the 2-cluster solution. This solution exists if $N$ is even and the coupling strengths satisfy*

$$g_{k-j} = g_{N-j}, \quad j = 1, \dots, k-1. \tag{16}$$

**Proof.** Using the same setup as in the previous section, we look for solution of the form (9)–(11). We assume $N = mkp$ and that coupling occurs between all neighbors from nearest to $k$th, i.e., the coupling matrix is defined by (15).

We consider an $m$-cluster solution as described by Eq. (11). Substituting this into Eq. (6) with the coupling matrix (15) gives

$$\begin{aligned}\omega &= g_1 H(\theta_{i+1,0} - \theta_{i0}) + g_2 H(\theta_{i+2,0} - \theta_{i0}) + \cdots + g_k H(\theta_{i+k,0} - \theta_{i0})\\ &\quad + g_{N-k}H(\theta_{i+N-k,0} - \theta_{i0}) + \cdots + g_{N-2}H(\theta_{i+N-2,0} - \theta_{i0})\\ &\quad + g_{N-1}H(\theta_{i+N-1,0} - \theta_{i0})\\ &= g_1 H(\phi_i) + g_2 H(\phi_{i+1} + \phi_i) + \cdots + g_k H\left(\sum_{j=0}^{k-1}\phi_{i+j}\right)\\ &\quad + g_{N-k}H\left(-\sum_{j=1}^{k}\phi_{i-j}\right) + \cdots + g_{N-2}H(-(\phi_{i-2} + \phi_{i-1}))\\ &\quad + g_{N-1}H(-\phi_{i-1}).\end{aligned}$$

There are $k$ cases to consider for the values of $\phi_i$, corresponding to $i = kq+1, kq+2, \dots, kq+k$. All must yield the same value of $\omega$ for the solution to exist. Thus we have

$$\begin{aligned}\omega &= g_1 H(0) + \cdots + g_{k-1}H(0) + g_k H(\psi_m) + g_{N-k}H(-\psi_m)\\ &\quad + g_{N-k+1}H(-\psi_m) + \cdots + g_{N-1}H(-\psi_m)\end{aligned} \tag{17}$$

$$= g_1 H(0) + \cdots + g_{k-2} H(0) + g_{k-1} H(\psi_m) + g_k H(\psi_m) + g_{N-k} H(-\psi_m) + g_{N-k+1} H(-\psi_m) + \cdots + g_{N-2} H(-\psi_m) + g_{N-1} H(0) \quad (18)$$

$$\vdots$$

$$= g_1 H(\psi_m) + \cdots + g_{k-1} H(\psi_m) + g_k H(\psi_m) + g_{N-k} H(-\psi_m) + g_{N-k+1} H(0) + \cdots + g_{N-1} H(0). \quad (19)$$

To proceed further, take the difference of Eqs. (17)–(18) to find the condition

$$[H(0) - H(\psi_m)]g_{k-1} + [H(-\psi_m) - H(0)]g_{N-1} = 0.$$

This will be satisfied for any $H$ if

$$\psi_m = \pi \text{ and } g_{k-1} = g_{N-1}.$$

Repeating this with other pairs of equations leads to the same constraint on $\psi_m$ and the conditions (16). The result follows. □

**Remark 3.1.** It follows from the proof of Theorem 3.1 that under the conditions (16) the $m$-cluster solution will exist if $H_{odd}(\psi_m) = 0$. Thus, we do not expect any $m$-cluster solution with $m > 2$ to exist for *every* $H$; however, solutions for specific $m$ may exist for a particular $H$. Further, other model-dependent solutions may exist under different conditions on the connection weights.

**Remark 3.2.** It follows from Eqs. (17)–(18) that the synchronous solution exists for any choice of coupling strengths. This is consistent with the results of [30]. Other types of model-independent cluster solutions, those where the cells in a cluster are not adjacent but dispersed through the network, may also exist [20,30].

According to (12), sufficient conditions for the 2-cluster solution described above to be asymptotically stable are $H'(0) > 0$, $H'(\pi) > 0$ and that the connectivity matrix $W$ defines a connected graph. To find necessary and sufficient conditions for stability, we consider an in-between case, where the additional connections $g_1, \dots, g_{k-1}, g_{N-k+1}, \dots, g_{N-1}$ are weaker than $g_k$ and $g_{N-k}$. We need to be careful that the weaker connections are not so weak that they are of similar strength to the neglected terms. Keeping in mind the conditions for existence of solutions derived above, we consider 2-cluster solutions ($m = 2$, $\psi_m = \pi$) and assume the coupling matrix defined by (15) satisfies the additional condition $g_1, \dots, g_{k-1}, g_{N-k+1}, \dots, g_{N-1} = s\,\delta$, while $g_k, g_{N-k} = O(1)$ with respect to $\epsilon$ and $0 < \epsilon \ll \delta \ll 1$. We show two examples in Fig. 2: $N = 8$ with $k = 2$ (Fig. 2(a)) and $N = 12$ with $k = 2$ (Fig. 2(b)). For the example with $N = 12$, the $O(1)$ couplings are the same as in Fig. 1(a) (represented by solid lines) with weaker couplings between nearest neighbors (represented by dashed lines).

We have the following result.

**Theorem 3.2** (*Balanced Additional Coupling*)**.** *Consider the model (6) with $N = 2kp$. Suppose the coupling matrix is defined by*

$$\text{circ}[0, \delta s, \dots, \delta s, g_k, 0, \dots, 0, g_{N-k}, \delta s, \dots, \delta s], \quad (20)$$

*where $s, g_j$ are positive, $g_k, g_{N-k} = O(1)$ with respect to $\epsilon$ and $s = O(1)$ with respect to $\delta$ and $0 < \epsilon \ll \delta \ll 1$. Then there is a 2-cluster solution where each cluster consists of $p$ subgroups of $k$ neurons. Each subgroup is synchronized and adjacent groups have phase difference $\pi$. This solution is locally asymptotically stable if and only if $H'(\pi) > 0$ and $H'(0)+H'(\pi) > 0$.*

**Proof. Existence.** The existence of solutions follows from Theorem 3.1 since the given $N$ and coupling strengths satisfy the conditions of that theorem.

**Stability.** A simple calculation shows that the Jacobian matrix for the linearization of the model (6) with the coupling matrix (20) about the solution (9)–(11) can be written as

$$\epsilon(A + s\delta B),$$

where $A$ is the Jacobian matrix for the situation with no additional coupling ($\delta = 0$). It follows from the discussion in Section 3.1 that $A$ has $k$ zero eigenvalues and the rest of the eigenvalues are proportional (with positive constant) to $-H'(\pi)$. Further, the eigenvalue 0 has geometric multiplicity $k$ with linearly independent eigenvectors $\mathbf{v}_0, \dots, \mathbf{v}_{k-1}$. We take $\mathbf{v}_0 = [1, 1, \dots, 1]^T$.

Consideration of Eq. (6) shows that each row sum of $A + s\delta B$ is 0. Thus, when $\delta \neq 0$, one zero eigenvalue persists since $[A + s\delta B]\mathbf{v}_0 = \mathbf{0}$.

Now let $\lambda_j$ be a nonzero eigenvalue of $A$ with eigenvector $\mathbf{v}_j$. Then

$$(A + s\delta B)\mathbf{v}_j = \lambda_j \mathbf{v}_j + s\delta B\mathbf{v}_j = \lambda_j \mathbf{v}_j + O(\delta).$$

Thus, to order $\delta$, $\lambda_j$ remains an eigenvalue for the solution. If $\lambda_j = 0$, however, we have

$$[A + s\delta B]\mathbf{v}_j = s\delta B\mathbf{v}_j, \ j = 1, \dots, k-1.$$

Thus the other zero eigenvalues may not persist.

For simplicity, in the rest of the proof we will take $k = 2$. The proof for other values of $k$ is similar. In this case

$$A = \text{circ}[-(g_2 + g_{N-2})H'(\pi),\ 0,\ g_2 H'(\pi),\ 0,\ \dots\ ,\ 0,\ g_{N-2}H'(\pi),\ 0],$$

and a second, linearly independent eigenvector of the eigenvalue 0 of $A$ is $\mathbf{v}_1 = [1, -1, 1, -1, \dots, 1, -1]^T$. Further, $B$ is a banded matrix with $B_{ii} = -(H'(0) + H'(\pi))$ and

$$B_{i,(i-1)\bmod N} = H'(\pi),\ B_{i,(i+1)\bmod N} = H'(0),\ \text{if } i \text{ even},$$
$$B_{i,(i-1)\bmod N} = H'(0),\ B_{i,(i+1)\bmod N} = H'(\pi),\ \text{if } i \text{ odd}.$$

It then follows that with $\delta > 0$ the second zero eigenvalue becomes $-2s\delta[H'(0)+H'(\pi)]$ since $[A+s\delta B]\mathbf{v}_1 = s\delta B\mathbf{v}_1 = -2s\delta[H'(0)+H'(\pi)]\mathbf{v}_1$.

In summary, all eigenvalues except the one zero eigenvalue that persists satisfy $\Re(\lambda_j) < 0$ if and only if $H'(\pi) > 0$ and $H'(0)+H'(\pi) > 0$.

Recall that the solutions we study are of the form $\bar{\theta}_i = (\Omega+\epsilon\omega)t+\theta_{i0}$. Thus the solutions correspond to lines

$$\theta_{(i+1)mod\,N} - \theta_i = \phi_i,$$

with $\phi_i$ given by (11). The zero eigenvalue that persists corresponds to motion along these lines and hence does not affect the stability of the solutions. The result follows. □

**Remark 3.3.** The key point of the proof is that if the additional couplings are of the appropriate strength $0 < \epsilon \ll \delta \ll 1$, then some of the eigenvalue structure in the case $\delta = 0$ is preserved. This enables us to obtain necessary and sufficient conditions for stability. If $\delta$ is larger this structure is lost, and necessary conditions are difficult to obtain.

**Remark 3.4.** Note that the necessary and sufficient conditions of Theorem 3.2 are more precise than the sufficient condition in (12) at the expense of the additional constraint on the coupling strengths as discussed above. In particular Theorem 3.2 shows that asymptotically stable 2-cluster solutions are possible if $H'(0) < 0$ but are not possible if $H'(\pi) < 0$.

**Remark 3.5.** It follows from Remark 3.1, that under the conditions of Theorem 3.2 other cluster solutions may exist for *particular* models. The proof of Theorem 3.2 shows that if these solutions are unstable for the case $\delta = 0$, then they will be unstable for the case $\delta > 0$ and sufficiently small.

### 3.2.1. Application to the model network

For comparison with the numerical simulations in the next section, we now apply the phase model results to the model network (8) with parameters as in Table 1 and symmetric coupling matrix defined by

$$\text{circ}[0, g_1, g_2, \dots, g_k, 0, \dots, 0, g_k, \dots, g_1]. \quad (21)$$

We assume that $g_k = O(1)$ with respect to $\epsilon$. We consider some examples with specific values for the total number of neurons $N$, with $N = mkp$ for some integers $m, k, p$ with $m > 1$.

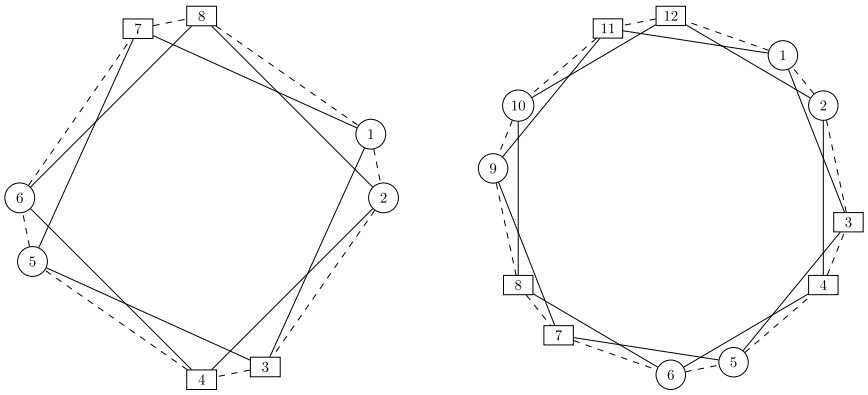


(a) (b)

**Fig. 2.** (a) Left: The network of $N = 8$ with additional coupling (in dashed lines) between nearest neighbors; (b) Right: The network of $N = 12$ with additional coupling between nearest neighbors.

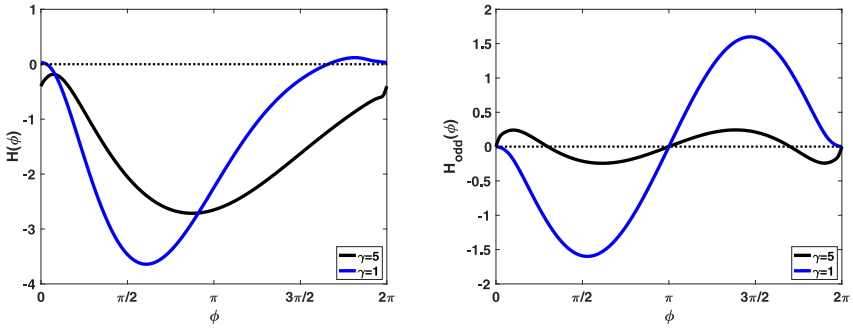


(a) The interaction function $H(\phi)$ (b) The odd part of the interaction function $H_{odd}(\phi)$

**Fig. 3.** Graphs of the interaction function $H$ for the phase model (6) corresponding to the neural model (8). All parameter values are given in Table 1 except the parameter $\gamma$ which is indicated.

To begin, we used XPPAUT [45] to numerically compute the functions $H$ and $H_{odd}$ for the model (8) with parameters given in Table 1 and two different values of the parameter $\gamma$. The results are shown in Fig. 3.

In [19] it is shown that the synchronous (1-cluster) solution exists for all values of $N$ and any circulant coupling matrix, and that this solution is asymptotically stable if $H'(0) > 0$ and unstable if $H'(0) < 0$. Thus from Fig. 3 we predict that, for the specific neural model we consider, given in Eq. (8), with any circulant coupling matrix, the synchronous solution is asymptotically stable if $\gamma = 5$ and unstable if $\gamma = 1$.

Now consider the case of decoupled networks. Given $N$ and $k$, the discussion of Section 3.1 gives the stability condition for any appropriate $m$-cluster solution. In the numerical simulations below we use symmetric coupling, $g_k = g_{N-k} > 0$, so the stability condition in Eq. (13) reduces to $H'_{odd}(\psi_m) > 0$, where $H_{odd}$ is the odd part of $H$ and $\psi_m$ is the phase difference between clusters as defined in the theorem. Thus to find the stability of an $m$-cluster solution, we need only calculate $\psi_m$ and determine the sign of $H'_{odd}(\psi_m)$. For example, consider $N = 8$ and $k = 2$. Then the possible $m$-cluster solutions with 2 adjacent neighbors synchronized correspond to $m = 2$ or $m = 4$. For $m = 2$, $\psi_m = \pi$ and for $m = 4$, $\psi_m = \pi/2$ or $\psi_m = 3\pi/2$. From Fig. 3 it is clear that (for both values of $\gamma$) $H'_{odd}(\pi) > 0$, $H'_{odd}(\pi/2) < 0$ and $H'_{odd}(3\pi/2) < 0$. Thus, for $N = 8$ with only second nearest neighbor coupling, the prediction is that the only stable solution with 2 adjacent neighbors synchronized is the 2-cluster solution. We summarize the predictions for other values of $N$ in the second last column of Table 2.

Finally, consider the case where the additional couplings are equal and of order $\delta$, $g_1 = g_2 = \cdots = g_{k-1} = s\delta$, where $\delta$ and $s$ are as in Theorem 3.2. (See Fig. 2 for examples with $N = 8$ or $N = 12$ and $k = 2$.) It follows from Theorem 3.1, that for $N = mkp$, the only cluster solutions with $k$ neighbors synchronized that will exist correspond to $m = 2$. Further, it follows from Theorem 3.2 if $N = 2kp$ the 2-cluster solution with $k$ nearest neighbors synchronized will exist and will be stable for both $\gamma = 1, 5$ since in both cases $H'(\pi) > 0$ and $H'(0) + H'(\pi) > 0$ from Fig. 3. These results are summarized in

**Table 2**
Existence and stability predictions from phase model analysis for $m$-cluster solutions with $k$ nearest neighbors synchronized in the network (8) with parameters given in Table 1.

| $N$ | $k$ | $m$ | $p$ | $\psi_m$ | Coupling | |
|---|---|---|---|---|---|---|
| | | | | | $k$ only | $1,\ldots,k$ |
| 8 | 2 | 2 | 2 | $\pi$ | Stable | Stable |
| | | 4 | 1 | $\pi/2,\ 3\pi/2$ | Unstable | DNE |
| | 4 | 2 | 1 | $\pi$ | Stable | Stable |
| 12 | 2 | 2 | 3 | $\pi$ | Stable | Stable |
| | | 3 | 2 | $2\pi/3,\ 4\pi/3$ | Stable | DNE |
| | | 6 | 1 | $\pi/3,\ 5\pi/3$ | Unstable | Unstable |
| | 3 | 2 | 2 | $\pi$ | Stable | Stable |
| | | 4 | 1 | $\pi/2,\ 3\pi/2$ | Unstable | DNE |
| 18 | 2 | 3 | 3 | $2\pi/3,\ 4\pi/3$ | Stable | DNE |
| | | 9 | 1 | $2\pi/9,\ 4\pi/9,\ 14\pi/9,\ 16\pi/9$ | Unstable | DNE |
| | | | | $8\pi/9,\ 10\pi/9$ | Stable | DNE |
| | 3 | 2 | 3 | $\pi$ | Stable | Stable |
| | | 3 | 2 | $2\pi/3,\ 4\pi/3$ | Stable | DNE |
| | | 6 | 1 | $\pi/3,\ 5\pi/3$ | Unstable | DNE |

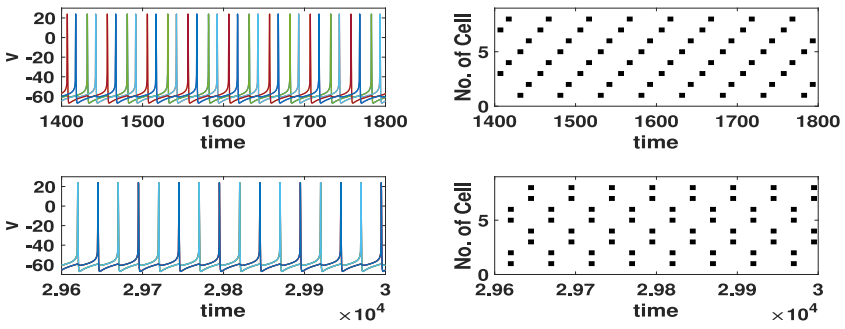


(a) Transition from 4-cluster (top) to 2-cluster solution for $N = 8$ with $k = 2$

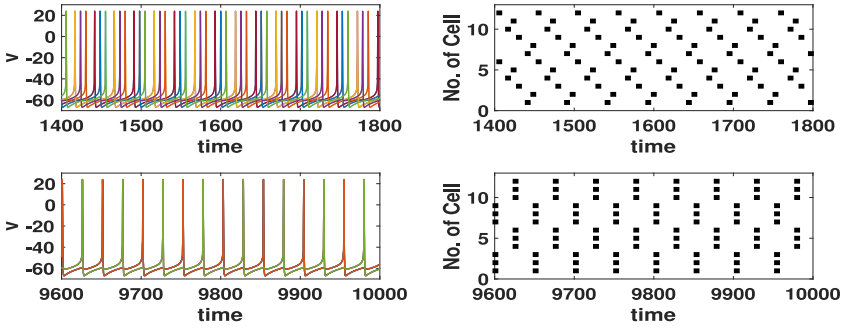


(b) Transition from 6-cluster (top) to 2-cluster solution for $N = 12$ and $\gamma = 5$ with $k = 3$

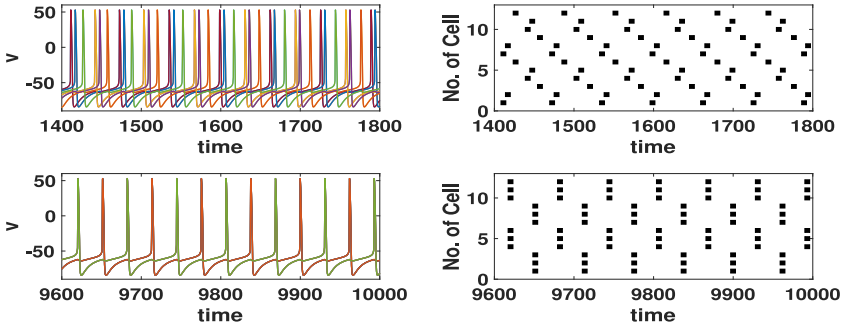


(c) Transition from 6-cluster (top) to 2-cluster solution for $N = 12$ and $\gamma = 1$ with $k = 3$

**Fig. 4.** (a) and (b): Time series (left) and its raster plot (right) to show a transition from cluster solutions consisting of non-spatially adjacent cells in each cluster to 2-cluster solutions with spatially adjacent cells in each cluster when additional coupling(s) are applied to be in the balanced regime as defined in Theorem 3.2. There are no additional coupling(s) for $0 \le t \le 1500$ ms, which is then set to 0.1 for $t > 1500$ ms; (c): the same transition shown as in (b) except the value of $\gamma = 1$ compared to $\gamma = 5$ in (b).

the last column of Table 2. Finally, note that in Fig. 3 for $\gamma = 5$ we have $H_{odd}(\phi) = 0$ at $\phi \approx \pi/3, 5\pi/3$. Thus from Remark 3.1, we predict that the 6-cluster solution may exist if $N = 6kp$. Since this solution is unstable for the case with no additional couplings (see second last column of Table 2), from Remark 3.5 we expect that it will be unstable with the additional couplings.

### 3.2.2. Existence of non-spatially adjacent cluster solutions

In this section, we consider the existence (or non-existence) of solutions of (6), with non-zero coupling between the first to $k$th nearest neighbors, that do not display synchronized firing between spatially adjacent cells. In particular, we consider the case when (11) is not satisfied but instead there are non-zero phase differences between spatially adjacent cells given by (14). With $g_1, g_2, \dots, g_k \neq 0$, the evolution equation for the phase differences $\phi_i$ derived from (6) becomes

$$\begin{aligned}\frac{d\phi_i}{dt} &= \epsilon \sum_{j=1}^{k} g_j \left[ H\left(\sum_{s=0}^{j-1} \phi_{i+s+1}\right) - H\left(\sum_{s=0}^{j-1} \phi_{i+s}\right) \right. \\ &\quad \left. + H\left(-\sum_{s=0}^{j-1} \phi_{i-s}\right) - H\left(-\sum_{s=0}^{j-1} \phi_{i-s-1}\right) \right].\end{aligned} \tag{22}$$

For simplicity, we consider the case $k = 2$. In this case, any equilibrium solution must satisfy the following equation:

$$\begin{aligned}0 &= \epsilon g_1 \left[ H\left(\phi_{i+1}\right) - H\left(\phi_i\right) + H\left(-\phi_i\right) - H\left(-\phi_{i-1}\right) \right] \\ &\quad + \epsilon g_2 \left[ H\left(\phi_{i+1} + \phi_{i+2}\right) - H\left(\phi_i + \phi_{i+1}\right) + H\left(-\phi_i - \phi_{i-1}\right) \right. \\ &\quad \left. - H\left(-\phi_{i-1} - \phi_{i-2}\right) \right],\end{aligned}$$

where $1 \le i \le N$. As described in Section 3.1, the solutions we consider satisfy $\phi_{2q+1} = \alpha$ and $\phi_{2q+2} = \pi - \alpha$ for $q = 0, 1, \dots, \frac{N}{2} - 1$ where $\alpha > 0$. Since this implies that $\phi_i + \phi_{i+1} = \pi$ for any $i \mod N$, it follows that the second term on the right-hand side will be zero. Thus, for existence, the first term must be zero, which reduces to

$$\begin{aligned}0 &= \epsilon g_1 [H(\pi - \alpha) - H(\alpha) + H(-\alpha) - H(-(\pi - \alpha))], \ i = 2q + 1, \\ 0 &= \epsilon g_1 [H(\alpha) - H(\pi - \alpha) + H(-(\pi - \alpha)) - H(-\alpha)], \ i = 2q + 2,\end{aligned} \tag{23}$$

for $q = 0, 1, \dots, \frac{N}{2} - 1$. Two conditions for which these equations are satisfied are: (i) for any time shift $\alpha$ if the function $H$ is even; and (ii) for $\alpha = \pi/2$ with any $H$. For most neural network models, $H$ is not an even function suggesting that the only time-shifted solution that may robustly exist has an $\alpha = \pi/2$ shift between cells $2q + 1$ and $2q + 2$ ($q = 0, 1, \dots, \frac{N}{2} - 1$) resulting in a 4-cluster solution with $\phi_i = \pi/2$ for

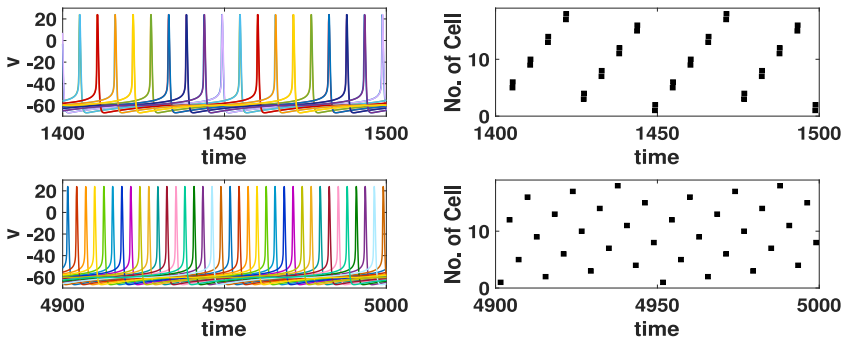


**Fig. 5.** Time series (left) and its raster plot (right) to show a transition from 9-cluster solution (top row) for a network of $N = 18$ with the second nearest coupling only ($k = 2$) consisting of spatially adjacent cells in each cluster to 18-cluster solution (bottom row) with the additional first nearest coupling. Additional coupling was applied at $t = 1500$.

all $i$. This is a cluster solution of the type studied in [19,20] where the neurons in a given cluster are not adjacent. Results in those papers show that this solution will be stable if and only if

$$g_1 H'_{odd}(\pi/2) + 2g_2 H'_{odd}(\pi)(1 + \cos(2j\pi/N)) > 0, \;\; j = 1, 2, \dots, N/2. \quad (24)$$

We note that since we always consider circulant coupling matrices, the system with $k$th nearest neighbor and additional coupling will admit $m$-cluster solutions of the type studied by [19,20,30]. Conditions for the stability of these solutions can be found in those papers.

Finally, for solutions with an arbitrary $\alpha$, existence will depend on the particular $H$ function for the model. As shown below, numerical results suggest that in model system (8) when $g_j = O(\epsilon)$ ($j = 1, \dots, k-1$) and $g_k = O(1)$ then solutions with $0 < \alpha \le \pi/2$ can exist. Intuitively, we may expect these solutions to exist and be stable since, to leading order in $\epsilon$, the system consists of decoupled subnetworks as in Section 3.1.

## 4. Numerical simulations

Here, we numerically explore the existence and stability of cluster solutions in networks of Wang–Buzsáki model neurons given by the system (8) with $O(\epsilon)$ coupling strength between $k$th nearest neighbor cells and additional coupling between first to $(k-1)$st nearest neighbors. To vary the strength of additional coupling(s) relative to the primary $k$th nearest neighbor coupling, $g_{syn}$, we introduce the scaling factor $\hat{w}_{ij}$ ($0 < \hat{w}_{ij} \le 1$) for $|i-j| \le k-1$, $i \ne j$ to multiply $W_{ij}$ in the system (8).

We first verify the existence and stability of clustered solutions with non-zero phase differences between adjacent cells, as given by (14), in networks when there is no additional coupling between first to $(k-1)$st nearest neighbors except the primary $k$th nearest neighbor coupling. We then show that the stability of the spatially adjacent cluster solutions is robust when the additional coupling is applied to be in the balanced regime, as considered in Theorem 3.2. In Fig. 4(a), we simulate a network of $N = 8$ neurons with second nearest coupling ($k = 2$) and varied values of the additional coupling between first nearest neighbors, as depicted in Fig. 2(a). We set the scaling factor $\hat{w}_{ij}$ ($|i-j| = 1$) for the first nearest neighbor coupling strength to zero until $t = 1500$ ms in the top row of Fig. 4(a). The resulting solution before $t = 1500$ ms shows a 4-cluster solution consisting of non-spatially adjacent cells in each cluster. In particular, the solution has similar phase differences ($\phi_i \approx \pi/2$, for $i = 1, 2, 3, 4$) between nearest neighbor cells. To test its existence and stability in the presence of balanced additional coupling(s), we set the scaling factor $\hat{w}_{ij}$ for the first nearest neighbor coupling strength from zero (Fig. 4(a), top row) to 0.1 at $t = 1500$ ms. Our results show that the solution eventually transitions to the stable 2-cluster solution with spatially adjacent cells in the clusters ($\phi_{2q+1} = 0$, $q = 0, 1, 2, 3$) (bottom row) which is predicted to be stable by Theorem 3.2.

As another example, we consider a network of $N = 12$ neurons with third nearest neighbor coupling ($k = 3$) and "balanced" first and second nearest neighbor couplings. Initially, the scaling factor $\hat{w}_{ij}$ ($|i-j| \le 2$) for the additional coupling is set to zero until $t = 1500$ ms. Results show a 6-cluster solution where clusters do not contain adjacent cells (Fig. 4(b), top row). However, when the scaling factor is increased to $\hat{w}_{ij} = 0.1$ ($|i-j| \le 2$) at $t = 1500$ ms, results show that the solution transitions to the stable 2-cluster solution (shown in bottom row) with clusters containing adjacent cells ($\phi_{3q+1} = \phi_{3q+2} = 0$, $q = 0, 1, 2, 3$) that is shown to be stable in Theorem 3.2.

Recall that Theorem 3.2 gives necessary and sufficient conditions for stability of the 2-cluster solution: $H'(\pi) > 0$ and $H'(0) + H'(\pi) > 0$, in contrast to the sufficient conditions for stability due to [28]: $H'(\pi) > 0$ and $H'(0) > 0$. The interaction function for our model with the standard parameters (black curves in Fig. 3) satisfies both conditions as $H'(0) > 0$. Changing the parameter $\gamma$ in Eq. (7) from 5 to 1, however, gives a function with $H'(0) < 0$ that still satisfies the condition $H'(0) + H'(\pi) > 0$ (blue curves in Fig. 3). Fig. 4(c) shows the same simulations as in Fig. 4(b) but with $\gamma = 1$. The results are the same as with $\gamma = 5$, agreeing with the results of Theorem 3.2 and highlighting the usefulness of the necessary and sufficient conditions.

We next show simulations suggesting that the 9-cluster solution for $N = 18$ which exists with only second nearest coupling ($k = 2$), shown in the top row of Fig. 5, no longer exists when the additional first nearest neighbor coupling is added. After $t = 1500$ ms, when the first nearest coupling is turned on, the 9-cluster solution transitions to the 18-cluster solution with equal phase difference between adjacent cells ($\phi_i = \pi/9$, for $i = 1, \dots, 18$, bottom row of Fig. 5). These simulation results agree with the result of Theorem 3.1, which states that the only $m$-cluster solution, with $k$ adjacent neurons synchronized, that can exist with additional nearest neighbor coupling is that for $m = 2$. Since for $N = 18$ and $k = 2$ the 2-cluster solution is never possible, no $m$-cluster solution with adjacent cells synchronized can occur. The network thus evolves to another solution type, namely the 18-cluster solution studied in [20] with equal phase differences between adjacent neurons. We have verified that this solution is predicted to be stable by phase model analysis [19,20].

Finally, we note that through our simulations we have found that other cluster solutions with synchronized neighbors that are not predicted by Theorem 3.1 may occur. Fig. 6 shows an example for a network with $N = 12$ where each neuron is connected to three of its neighbors ($k = 3$) in the strong coupling regime, $\hat{w}_{ij} = 1$ ($|i-j| \le 2$). This simulation shows a stable 2-cluster solution consisting of 3 groups of 2 synchronized adjacent neighbors.

## 5. Discussion

In this paper, we study 1-D, weakly coupled inhibitory neuron networks to investigate the existence and stability of $m$-cluster solutions, in which clusters consist of groups of adjacent cells in the network that fire together. To simply describe non-monotonic, distance-dependent connectivity [39], we first consider $k$th nearest neighbor symmetric coupling such that each neuron in the 1-D ring is connected with

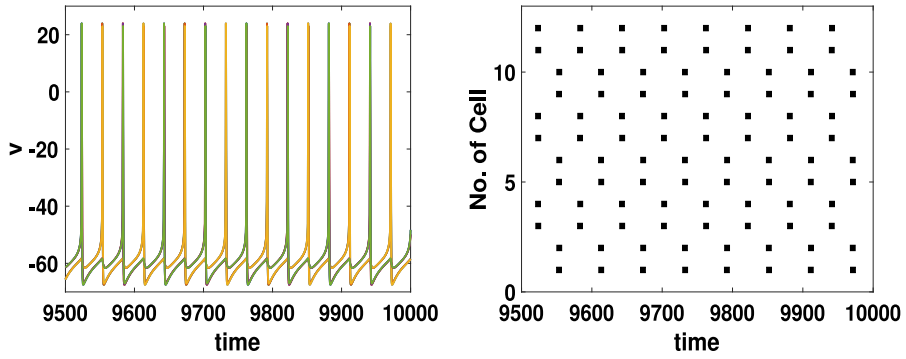


**Fig. 6.** Time series (left) and its raster plot (right) to show a 2-cluster solution for a network of $N = 12$ with $k = 3$ and strong additional first and second nearest couplings. The cluster solution consists of 3 groups of 2 synchronized adjacent cells in each cluster.

its $k$th nearest neighbors only. This connectivity scheme results in the decomposition of the network into $k$ disjoint subnetworks, and existence and stability conditions of $m$-cluster solutions depends on existence and stability of $m$-cluster solutions in each subnetwork where adjacent neurons have a phase difference of $2\pi/m$. These solutions, however, are not asymptotically stable as small perturbations disrupt synchrony among the subnetworks.

To study more generalized distance-dependent coupling, we consider the case where the network has coupling between the first to $k$th nearest neighbors. For strong enough additional coupling (first to $(k-1)$st nearest neighbor), only two of the spatially localized $m$-cluster solutions are guaranteed to persist for any model network. The synchronous (1-cluster) solution exists for any size of network and the 2-cluster solution exists if the network has an even number of neurons. We provide stability conditions for these two solutions. These results are confirmed with numerical simulations.

When the additional coupling is in a balanced regime (greater than $O(\epsilon)$ but less than $O(1)$ relative to the $k$th nearest neighbor coupling), we provide a new necessary and sufficient condition for stability of spatially localized, $m$-cluster solutions. We confirm these results with numerical simulations that highlight the dependence on the strength of the additional coupling for stability of these solutions. Specifically, numerical results show that with no or very weak additional coupling (closer to $O(\epsilon)$), solutions with more clusters exist but cells in the same cluster are spatially dispersed in the network. These solutions correspond to non-zero time-shifted solutions that are found in networks with only $k$th nearest neighbor coupling due to the decomposition of the network into disjoint subnetworks. In these solutions, the disjoint subnetworks are not synchronized so their cells fire with a non-zero time shift. However, when the additional balanced coupling is introduced to the network, solutions transition to the spatially localized $m$-cluster solutions.

This study extends our previous work [20] in that the existence and stability conditions of $m$-cluster solutions include $k$th nearest neighbor coupling with asymmetric weights. Previously, we only worked with a symmetric connectivity matrix for neurons that are coupled to their first and/or second nearest neighbors on both sides. Here, we also perform a perturbation analysis to discuss the existence and stability conditions with additional coupling(s) to the $k$th nearest coupling. Moreover, we extend our previous work by considering nonuniform phase differences between nearest neighbors.

**Model limitations and future directions.** Despite the richness of our analytical and numerical results, our results are based on the phase model reduction of an inhibitory network which explicitly assumes that neurons are weakly coupled to each other. Phase models have limitations even for studying networks of oscillatory neurons [46,47].

Synchronization in inhibitory networks can also be obtained by mechanisms known as Interneuron Network Gamma (ING) or Pyramidal Interneuron Network Gamma (PING) [48–52]. In these mechanisms, synchronization of inhibitory neurons results due to gating of the timing of firing by synaptic inhibition such that cells are suppressed while inhibitory synaptic currents are active and are able to fire when synaptic currents decay. Thus, this mechanism assumes sufficiently strong synaptic coupling between cells so as to prevent firing. Our results apply to the case of weak coupling in the inhibitory network where synaptic interactions perturb the timing of cell firing without suppression of firing.

Our results focus on 1-D networks whereas the recent study [39] on non-monotonic distance-dependent connectivity considered a 2-D network. Thus, our future study would extend the 1-D network model to investigate the 2-D network behaviors. In the 2-D setting, the diagonal neighbor coupling is a feature which could not be considered in our 1-D model. Thus we will consider its effects on cluster formation in 2-D inhibitory networks in conjunction with non-monotonic distance-dependent network connectivity.

**Conclusions.** Our work may help understand cluster formation in the striatum [1,38]. Note that the striatum has sparse, weak, unidirectional coupling [12]. Our results show that spatially localized clusters can occur when there are very few connections in the network. There has been some dispute as to whether clusters in the striatum are truly spatially compact, that is, involve only nearby neurons [38]. Our work shows that spatially compact clusters may occur, but that clusters which involve multiple groups of nearby neurons may also occur. Such solutions could correspond to clusters that involve both localized and longer range correlations between neurons as observed in [38]. Here we use reciprocal coupling in our simulations, but the mathematical results would apply to unidirectional coupling by setting some connections to zero. For example, in the decoupled networks case, clustered solutions can be found if $g_k > 0$ and $g_{N-k} = 0$. Since we use a general interaction function $H$, the mathematical results also apply to excitatory neurons so could be used to study cluster formation in the dentate gyrus [6].

## CRediT authorship contribution statement

**Hwayeon Ryu:** Conceptualization, Methodology, Writing - original draft, Writing - review & editing, Implemented and conducted numerical simulations. **Jennifer Miller:** Conceptualization, Methodology, Writing - original draft, Writing - review & editing, Conducted the phase model analyses. **Zeynep Teymuroglu:** Conceptualization, Methodology, Writing - original draft, Writing - review & editing, Conducted the phase model analyses. **Xueying Wang:** Conceptualization, Methodology, Writing - original draft, Writing - review & editing, Conducted the phase model analyses. **Victoria Booth:** Conceptualization, Methodology, Writing - original draft, Writing - review & editing, Implemented and conducted numerical simulations. **Sue Ann Campbell:** Conceptualization, Methodology, Writing - original draft, Writing - review & editing, Conducted the phase model analyses.

## Declaration of competing interest

The authors declare that they have no known competing financial interests or personal relationships that could have appeared to influence the work reported in this paper.

## Acknowledgments

We thank the American Institute of Mathematics for providing support through its Structured Quartet Research Ensembles program, from which this work was first initiated. Sue Ann Campbell acknowledges the support of the Natural Sciences and Engineering Research Council of Canada. The authors also thank the anonymous reviewers for helpful suggestions.

## References

[1] G. Barbera, B. Liang, L. Zhang, C.R. Gerfen, E. Culurciello, R. Chen, Y. Li, D.-T. Lin, Spatially compact neural clusters in the dorsal striatum encode locomotion relevant information, Neuron 92 (1) (2016) 202–213.
[2] G. Dragoi, G. Buzsáki, Temporal encoding of place sequences by hippocampal cell assemblies, Neuron 50 (1) (2006) 145–157.
[3] C.M. Gray, P. Koening, G. Engel, W. Singer, Oscillatory responses in cat visual cortex exhibit inter-columnar synchronization which reflects global stimulus properties, Nature 338 (6213) (1989) 334–337.
[4] K. Harris, J. Csicsvari, H. Hirase, G. Dragoi, G. Buzsáki, Organization of cell assemblies in the hippocampus, Nature 424 (6948) (2003) 552–556.
[5] G. Laurent, H. Davidowitz, Encoding of olfactory information with oscillating neural assemblies, Science 265 (5180) (1994) 1872–1875.
[6] S.F. Muldoon, I. Soltesz, R. Cossart, Spatially clustered neuronal assemblies comprise the microstructure of synchrony in chronically epileptic networks, Proc. Natl. Acad. Sci. 110 (9) (2013) 3567–3572.
[7] A. Adler, I. Finkes, S. Katabi, Y. Prut, H. Bergman, Encoding by synchronization in the primate striatum, J. Neurosci. 33 (11) (2013) 4854–4866.
[8] L. Carrillo-Reid, F. Tecuapetla, D. Tapia, A. Hernández-Cruz, E. Galarraga, R. Drucker-Colin, J. Bargas, Encoding network states by striatal cell assemblies, J. Neurophysiol. 99 (3) (2008) 1435–1450.
[9] A.K. Engel, P. Fries, W. Singer, Dynamic predictions: oscillations and synchrony in top-down processing, Nat. Rev. Neurosci. 2 (10) (2001) 704–716.
[10] R.F. Galán, G.B. Ermentrout, N.N. Urban, Predicting synchronized neural assemblies from experimentally estimated phase-resetting curves, Neurocomputing 69 (10) (2006) 1112–1115.
[11] S. Achuthan, C.C. Canavier, Phase-resetting curves determine synchronization, phase locking, and clustering in networks of neural oscillators, J. Neurosci. 29 (16) (2009) 5218–5233.
[12] D. Angulo-Garcia, J.D. Berke, A. Torcini, Cell assembly dynamics of sparsely-connected inhibitory networks: a simple model for the collective activity of striatal projection neurons, PLoS Comput. Biol. 12 (2) (2016) e1004778.
[13] C.C. Canavier, F.G. Kazanci, A.A. Prinz, Phase resetting curves allow for simple and accurate prediction of robust n: 1 phase locking for strongly coupled neural oscillators, Biophys. J. 97 (1) (2009) 59–73.
[14] D. Golomb, D. Hansel, B. Shraiman, H. Sompolinsky, Clustering in globally coupled phase oscillators, Phys. Rev. A 45 (6) (1992) 3516.
[15] D. Golomb, J. Rinzel, Clustering in globally coupled inhibitory neurons, Physica D 72 (3) (1994) 259–282.
[16] Z.P. Kilpatrick, B. Ermentrout, Sparse gamma rhythms arising through clustering in adapting neuronal networks, PLoS Comput. Biol. 7 (11) (2011) e1002281.
[17] Y.-X. Li, Y.-Q. Wang, R. Miura, Clustering in small networks of excitatory neurons with heterogeneous coupling strengths, J. Comput. Neurosci. 14 (2003) 139–159.
[18] A. Ponzi, J. Wickens, Sequentially switching cell assemblies in random inhibitory networks of spiking neurons in the striatum, J. Neurosci. 30 (17) (2010) 5894–5911.
[19] S.A. Campbell, Z. Wang, Phase models and clustering in networks of oscillators with delayed coupling, Physica D 363 (2018) 44–55.
[20] J. Miller, H. Ryu, Z. Teymuroglu, X. Wang, V. Booth, S.A. Campbell, Clustering in inhibitory neural networks with nearest neighbor coupling, in: T. Jackson, A. Radunskaya (Eds.), Applications of Dynamical Systems in Biology and Medicine, Springer, New York, 2015, pp. 99–121.
[21] F. Hoppensteadt, E. Izhikevich, Weakly Connected Neural Networks, Springer–Verlag, New York, 1997.
[22] M. Schwemmer, T. Lewis, The theory of weakly coupled oscillators, in: N. Schultheiss, A. Prinz, R. Butera (Eds.), Phase Response Curves in Neuroscience, Springer, New York, NY, 2012, pp. 3–31.
[23] P. Ashwin, J.W. Swift, The dynamics of n weakly coupled identical oscillators, J. Nonlinear Sci. 2 (1992) 69–108.
[24] K. Okuda, Variety and generality of clustering in globally coupled oscillators, Physica D 63 (1993) 424–436.
[25] N. Kopell, G. Ermentrout, Mechanisms of phase–locking and frequency control in pairs of coupled neural oscillators, in: B. Fiedler (Ed.), Handbook of Dynamical Systems, Vol 2: Toward Applications, Elsevier, Amsterdam, 2002, pp. 3–54.
[26] F. Saraga, L. Ng, F.K. Skinner, Distal gap junctions and active dendrites can tune network dynamics, J. Neurophysiol. 95 (3) (2006) 1669–1682.
[27] J.G. Mancilla, T.J. Lewis, D.J. Pinto, J. Rinzel, B.W. Connors, Synchronization of electrically coupled pairs of inhibitory interneurons in neocortex, J. Neurosci. 27 (8) (2007) 2058–2073.
[28] G.B. Ermentrout, Stable periodic solutions to discrete and continuum arrays of weakly coupled nonlinear oscillators, SIAM J. Appl. Math. 52 (6) (1992) 1665–1687.
[29] S.H. Strogatz, From kuramoto to crawford: exploring the onset of synchronization in populations of coupled oscillators, Physica D 143 (1–4) (2000) 1–20.
[30] D.A. Wiley, S.H. Strogatz, M. Girvan, The size of the sync basin, Chaos 16 (1) (2006) 015103.
[31] F.G. Kazanci, B. Ermentrout, Pattern formation in an array of oscillators with electrical and chemical coupling, SIAM J. Appl. Math. 67 (2) (2007) 512–529.
[32] T. Girnyk, M. Hasler, Y. Maistrenko, Multistability of twisted states in non-locally coupled kuramoto-type models, Chaos 22 (1) (2012) 013114.
[33] S. Heitmann, G.B. Ermentrout, Synchrony, waves and ripple in spatially coupled kuramoto oscillators with mexican hat connectivity, Biol. Cybern. 109 (3) (2015) 333–347.
[34] H. Sakaguchi, Y. Kuramoto, A soluble active rotater model showing phase transitions via mutual entertainment, Progr. Theoret. Phys. 76 (3) (1986) 576–581.
[35] D. Hansel, G. Mato, C. Meunier, Clustering and slow switching in globally coupled phase oscillators, Phys. Rev. E 48 (5) (1993) 3470.
[36] F.G. Kazanci, B. Ermentrout, Wave formation through the interactions between clustered states and local coupling in arrays of neural oscillators, SIAM J. Appl. Dyn. Syst. 7 (2) (2008) 491–509.
[37] B. Miller, A. Walker, A. Shah, S. Barton, G. Rebec, Dysregulated information processing by medium spiny neurons in striatum of freely behaving mouse models of huntington's disease, J. Neurophysiol. 100 (2008) 2205–2216.
[38] A. Klaus, G.J. Martins, V.B. Paixao, P. Zhou, L. Paninski, R.M. Costa, The spatiotemporal organization of the striatum encodes action space, Neuron 95 (5) (2017) 1171–1180.
[39] S. Spreizer, M. Angelhuber, J. Bahuguna, A. Aertsen, A. Kumar, Activity dynamics and signal representation in a striatal network model with distance-dependent connectivity, Eneuro 4 (4) (2017).
[40] G. Ermentrout, D. Terman, Mathematical Foundations of Neuroscience, Springer, New York, NY, 2010.
[41] X.-J. Wang, G. Buzsáki, Gamma oscillation by synaptic inhibition in a hippocampal interneuronal network model, J. Neurosci. 16 (1996) 6402–6413.
[42] A. Hodgkin, A. Huxley, A quantitative description of membrane current and its application to conduction and excitation in nerve, J. Physiol. 117 (1952) 500–544.
[43] J.-C. Lacaille, S. Williams, Membrane properties of interneurons in stratum oriens-alveus of the CA1 region of rat hippocampus in vitro, Neuroscience 36 (2) (1990) 349–359.
[44] A. Destexhe, Z. Mainen, T. Sejnowski, Kinetic models of synaptic transmission, in: C. Koch, I. Segev (Eds.), Methods in Neuronal Modeling: From Synapses to Networks, MIT Press, Cambridge, MA, 1998, pp. 1–25.
[45] B. Ermentrout, Simulating, Analyzing, and Animating Dynamical Systems: a Guide to XPPAUT for Researchers and Students, Vol. 14, SIAM, 2002.
[46] K.C. Wedgwood, K.K. Lin, R. Thul, S. Coombes, Phase-amplitude descriptions of neural oscillator models, J. Math. Neurosci. 3 (1) (2013) 2.
[47] P. Ashwin, S. Coombes, R. Nicks, Mathematical frameworks for oscillatory network dynamics in neuroscience, J. Math. Neurosci. 6 (1) (2016) 2.
[48] M. Whittington, R.D. Traub, N. Kopell, B. Ermentrout, E. Buhl, Inhibition-based rhythms: experimental and mathematical observations on network dynamics, Int. J. Psychophysiol. 38 (3) (2000) 315–336.
[49] N. Kopell, D. Borgers, P. Malerba, A. Tort, Gamma and theta rhythms in biophysical models of hippocampal circuits, in: V. Cutsuridis, B. Graham, S. Cobb, I. Vida (Eds.), Microcircuits, a Computational Modeler'S Resource Book, Springer, New York, NY, 2010, pp. 423–457.
[50] P. Tiesinga, T.J. Sejnowski, Cortical enlightenment: Are attentional gamma oscillations driven by ING or PING?, Neuron 63 (6) (2009) 727–732.
[51] X.-J. Wang, Neurophysiological and computational principles of cortical rhythms in cognition, Physiol. Rev. 90 (3) (2010) 1195–1268.
[52] S. Rich, V. Booth, M. Zochowski, Intrinsic cellular properties and connectivity density determine variable clustering patterns in randomly connected inhibitory neural networks, Front. Neural Circuits 10 (2016) 82.